

Dynamical Manifestations of Quantum Chaos: Correlation Hole and Bulge

E. J. Torres-Herrera¹ and Lea F. Santos²

¹*Instituto de Física, Benemérita Universidad Autónoma de Puebla,
Apt. Postal J-48, Puebla, Puebla, 72570, Mexico*

²*Department of Physics, Yeshiva University, New York, New York 10016, USA*

A main feature of a chaotic quantum system is a rigid spectrum where the levels do not cross. We discuss how the presence of level repulsion in lattice many-body quantum systems can be detected from the analysis of their time evolution instead of their energy spectra. This approach is advantageous to experiments that deal with dynamics, but have limited or no direct access to spectroscopy. Avoided crossings are manifested at long times by a drop, referred to as correlation hole, below the asymptotic value of the survival probability and by a bulge above the saturation point of the von Neumann entanglement entropy and the Shannon information entropy. In contrast, the evolution of these dynamical quantities at shorter times reflect the level of delocalization of the initial state, but not necessarily a rigid spectrum. The correlation hole is a general indicator of the integrable-chaos transition in disordered and clean models and as such can be used to detect the transition to the many-body localized phase in disordered interacting systems.

Keywords: quench dynamics, level repulsion, power-law decay

I. INTRODUCTION

Quantum chaos refers to specific properties of the spectrum and the eigenstates of a system, most notably to correlations between the eigenvalues that result in avoided crossings [1–5]. In the context of nuclear physics, the analysis of the statistical properties of the spectrum dates back to Wigner’s works [6, 7] and was soon extended to other complex systems, such atoms, molecules and condensed matter models. From a dynamical perspective, the onset of quantum chaos has been associated with very fast relaxation processes. Nevertheless, fast equilibration is found also in non-chaotic systems. This paper is devoted to the description of dynamical quantities that can unambiguously identify the presence of level repulsion in lattice many-body quantum systems.

In an attempt to distinguish quantum motion in chaotic and regular systems, Peres [8] argued that after the saturation of the Loschmidt echo, the fluctuations in chaotic models should be smaller than in regular systems. More recently, however, it has been shown that the amplitudes of the fluctuations after equilibration decrease with system size in a very similar way for chaotic and also integrable systems with interactions [9–12]. Comparisons between infinite-time averages and thermodynamic averages have also been used to determine the onset of thermalization and by extension of quantum chaos [13, 14], although the results depend on the initial state [15, 16] and at high energies level repulsion may in fact not be essential. In contrast to these approaches, we focus here on evident manifestations of avoided crossings that can emerge before the equilibration of the system.

Quantum chaos has been linked with the linear growth in time of the von Neumann entanglement entropy up to saturation [17]. This behavior is analogous to what happens to the Shannon information entropy [18, 19], which has the advantage of being computationally less expensive. However, the linear growth of entropies is observed also in interacting integrable models [18–22]. Similarly, quantum chaos has been connected with the initial exponential decay of the survival probability and Loschmidt echo [23–26], but the same is verified in integrable models [27] and decays even faster are found in both regimes [28–33].

In interacting systems with onsite disorder, localization due to large disorder occurs in parallel with the disappearance of level repulsion. Dynamical features at the vicinity of the delocalized-localized transition, which encompass the logarithmic growth of both entanglement and Shannon entropies [19, 34–36] and the power-law decay of the survival probability with exponents smaller than 1 [19, 37, 38], may then be taken as signatures of the chaos-integrable transition. But this is a very particular example, where both transitions coincide. We seek for means to differentiate chaos from integrability in general scenarios, including also clean models and the spatially delocalized phases of disordered systems.

The power-law decay of the survival probability at long times is not exclusive to systems in the vicinity of the transition to the localized phase. This behavior is inevitable in any quantum system, but its origins as well as the values of the power-law exponents vary [39, 40]. One ever-present cause of power-law decays is the unavoidable bounds in the energy spectrum of quantum systems [41, 42]. In lattice many-body quantum systems with two-body interactions, this leads to exponents close to 2 [39, 40]. Such large exponents indicate chaotic initial states and anticipate thermalization [39, 40], but they are still not explicit signatures of level repulsion.

Unambiguous dynamical manifestations of level repulsion happen at yet longer times, of the order of (but smaller than) the inverse of the mean level spacing. It shows up in the form of a drop in the value of the survival probability

below its saturation point, a phenomenon known as correlation hole [43]. As we discuss here, it also leads to a minor bulge above the saturation values of the Shannon and entanglement entropies. The correlation hole reflects the long-range correlations of the eigenvalues of complex systems. It is the dip of the spectral form factor discussed in [44]. It has also been investigated in molecules [43, 45–49], random matrices [50–54] and microwave billiards [55, 56]. Here, we extend these studies to clean and disordered spin-1/2 models.

We stress that in this work we equate the term quantum chaos with level repulsion, more precisely with the Wigner-Dyson distribution of the spacings between neighboring levels [1–3]. An alternative approach is to view quantum chaos as the emergence of chaotic eigenstates. The latter refers to states with a very large number of uncorrelated components, which may occur even in systems that do not show level repulsion [13]. This leads to generic dynamical behaviors that exhibit very fast relaxation processes. This second viewpoint is inspired by early works from Chirikov [57, 58].

This paper is organized as follows. Section 3 presents the models and dynamical quantities studied. Section 4 compares the dynamics of integrable and chaotic clean models, using for that the evolution of the entanglement entropy, the Shannon entropy, and the survival probability. Section 5 shows how the correlation hole can be used to indicate the transition to a many-body localized phase. Conclusions are presented in Sec. 6.

II. SPIN-1/2 MODELS AND QUANTITIES ANALYZED

We investigate a one-dimensional spin-1/2 system with an even number L of sites. The Hamiltonian is given by

$$\begin{aligned} H = & \varepsilon_1 JS_1^z + \varepsilon_L JS_L^z + dJS_{L/2}^z + \sum_{k=1}^L h_k S_k^z \\ & + J \sum_k (S_k^x S_{k+1}^x + S_k^y S_{k+1}^y + \Delta S_k^z S_{k+1}^z) \\ & + \lambda J \sum_k (S_k^x S_{k+2}^x + S_k^y S_{k+2}^y + \Delta S_k^z S_{k+2}^z). \end{aligned} \quad (1)$$

Above, $\hbar = 1$ and $S_k^{x,y,z} = \sigma_k^{x,y,z}/2$ are spin operators acting on site k , $\sigma_k^{x,y,z}$ being Pauli matrices. Three defects are created by applying three different local static magnetic fields in the z -direction on the first, last, and middle sites. These fields lead, respectively, to the following Zeeman splittings: $\varepsilon_1 J$, $\varepsilon_L J$, and dJ . The amplitudes h_k correspond to on-site disorder; they are random numbers from a uniform distribution in $[-h, h]$. The second line in Eq. (1) represents the couplings between nearest neighbors (NN). They include the flip-flop term $S_k^x S_{k+1}^x + S_k^y S_{k+1}^y$ and the Ising interaction $S_k^z S_{k+1}^z$. The third line corresponds to the couplings between next-nearest neighbors (NNN). J is the exchange coupling, Δ is the anisotropy parameter, and λ is the ratio between NN and NNN couplings. We set $J = 1$. The sum in the second (third) line runs up to $L - 1$ ($L - 2$) for open boundary conditions and up to L for closed boundaries.

Hamiltonian (1) conserves the total spin in the z -direction, $S^z = \sum_{k=1}^L S_k^z$, so $[H, S^z] = 0$. We deal with the sector that has $L/2$ up-spins and dimension $\mathcal{D} = L!/[(L/2)!]^2$.

The purpose of the defects on site 1 and site L is to reduce finite size effects and break symmetries, such as parity, conservation of total spin, and spin reversal. We consider $\varepsilon_1, \varepsilon_L$ as small random numbers from a uniform distribution in the interval $[-0.1, 0.1]$.

1. Clean and Disordered Models

In Sec. III, the results for three models with $\varepsilon_1, \varepsilon_L \neq 0$, $h = 0$, and open boundary conditions are compared.

(i) For $\Delta \neq 0$ and $d, \lambda = 0$, Eq. (1) corresponds to the integrable **XXZ model**. Notice that the integrability is not broken by the addition of border defects [59]. We choose $\Delta = 0.48$. The level spacing distribution in this case is Poisson, as typical of integrable models, where the eigenvalues are uncorrelated and crossings are not prohibited.

(ii) The system becomes chaotic and shows a Wigner-Dyson distribution when $d \lesssim 1$ [60, 61]. We fix $d = 0.9$ and $\lambda = 0$ and refer to it as the **defect model**.

(iii) Chaos also emerges when $\lambda \lesssim 1$ [62–65]. We choose $\lambda = 1$ and $d = 0$ and denote this case as the **NNN model**.

Disordered model: In Sec. IV, we study the disordered spin-1/2 model with $h \neq 0$, $\Delta = 1$, $\varepsilon_1, \varepsilon_L, d, \lambda = 0$, and periodic boundary conditions. As h increases from zero to $h \lesssim 1$, the level spacing distribution changes from Poisson

to Wigner-Dyson [60, 66] and the eigenstates become even more delocalized in space [67]. As the disorder strength is further increased, the distribution transitions from Wigner-Dyson back to Poisson and the eigenstates become more localized [60, 67, 68].

2. Basis and Initial States

When studying localization in space, it is natural to choose the site-basis vectors, as we do in this work. They are also known in quantum information theory as computational-basis vectors. These states have on each site a spin that either points up or down in the z -direction, as for example $|\downarrow\uparrow\downarrow\uparrow\downarrow\uparrow\downarrow\uparrow\dots\rangle_z$. We notice, however, that further insights on the interplay between interaction and disorder may be gained by analyzing the eigenstates also in other basis vectors, such as those corresponding to the eigenstates of the XXZ model [68].

The site-basis vectors are denoted by $|\phi_n\rangle$. They are the initial states, $|\Psi(0)\rangle = |\phi_{n=ini}\rangle$, that we use in the analysis of the system dynamics.

A. Entanglement Entropy

The von Neumann entanglement entropy, S_{vN} , is obtained by separating the system in subsystems A and B and then performing the partial trace of one of the two [69]. The entanglement entropy is the von Neumann entropy of the reduced density matrix $\rho_A = \text{Tr}_B[\rho]$, where ρ is the density matrix of the total system. We divide the chain in two equal sizes, so the dimension of ρ_A is $\mathcal{D}_A = 2^{L/2}$.

The system is initially in the product state $\rho(0) = |\Psi(0)\rangle\langle\Psi(0)| = |\phi_{ini}\rangle\langle\phi_{ini}|$, so $S_{vN}(0) = 0$. As time passes, the amount of entanglement grows as quantified by

$$S_{vN}(t) = -\text{Tr}[\rho_A(t) \ln \rho_A(t)]. \quad (2)$$

B. Shannon Entropy

The Shannon information entropy, S_{Sh} , is often used to measure the level of delocalization of the eigenstates in a chosen basis [4]. It can also be used to quantify the spreading in time of the initial state on a selected basis. For the site-basis vectors, it is written as

$$S_{Sh}(t) = -\sum_{n=1}^{\mathcal{D}} P_n(t) \ln P_n(t), \quad (3)$$

where $P_n(t) = |\langle\phi_n|e^{-iHt}|\phi_{ini}\rangle|^2$ and \mathcal{D} is the dimension of the subspace considered.

C. Survival Probability and Correlation Hole

The survival probability, $P_{ini} = |\langle\Psi(0)|\Psi(t)\rangle|^2$, is the probability for finding the initial state later in time. For $|\Psi(0)\rangle = |\phi_{ini}\rangle$, it is given by

$$P_{ini}(t) = |\langle\phi_{ini}|e^{-iHt}|\phi_{ini}\rangle|^2 = \left| \sum_{\alpha} |C_{ini}^{(\alpha)}|^2 e^{-iE_{\alpha}t} \right|^2 = \left| \int \rho_{ini}(E) e^{-iEt} dE \right|^2, \quad (4)$$

where $C_{ini}^{(\alpha)} = \langle\psi_{\alpha}|\phi_{ini}\rangle$ is the overlap between the initial state and the eigenstates $|\psi_{\alpha}\rangle$ of the Hamiltonian H that evolves $|\Psi(0)\rangle$, E_{α} are the eigenvalues of H , and $\rho_{ini}(E) = \sum_{\alpha} |C_{ini}^{(\alpha)}|^2 \delta(E - E_{\alpha})$ is the energy distribution weighted by the components $|C_{ini}^{(\alpha)}|^2$ of the initial state $|\Psi(0)\rangle$. This distribution is known as the local density of states (LDOS) or strength function.

The survival probability is the absolute square of the Fourier transform of the LDOS. If one has detailed information about the LDOS, one should be able to predict the dynamics. Equivalently, $P_{ini}(t)$ is the Fourier transform of the

spectral autocorrelation function, $G(E)$, that is

$$P_{ini}(t) = \int G(E) e^{-iEt} dE, \quad (5)$$

$$G(E) = \sum_{\alpha} |C_{ini}^{(\alpha)}|^4 \delta(E - E_{\alpha}) + \sum_{\beta \neq \alpha} |C_{ini}^{(\beta)}|^2 |C_{ini}^{(\alpha)}|^2 \delta(E - (E_{\alpha} - E_{\beta})). \quad (6)$$

It is clear from Eqs. (5) and (6) that the dephasing of the initial state depends on both the initial state, through the overlaps $|C_{ini}^{(\alpha)}|^2$, and the spacings between all energy levels.

The first term of $G(E)$ leads to the infinite time average of the survival probability $\overline{P_{ini}} = \sum_{\alpha} |C_{ini}^{(\alpha)}|^4$. It is larger than zero in finite systems. The lowest values are reached by full random matrices (FRM), which are matrices filled with random numbers whose sole constraint is to satisfy the symmetries of the system they represent [3]. For FRM of Gaussian Orthogonal Ensembles (GOE), $\overline{P_{ini}} \simeq 3/\mathcal{D}$ [4, 18], where \mathcal{D} is the dimension of the matrix.

The second term of $G(E)$ determines the decay of $P_{ini}(t)$. In FRM, it factorizes into a term depending only on the overlaps and one depending on the eigenvalues, as

$$\sum_{\beta \neq \alpha} \left\langle |C_{ini}^{(\beta)}|^2 |C_{ini}^{(\alpha)}|^2 \right\rangle_{FRM} \langle \delta(E - (E_{\alpha} - E_{\beta})) \rangle_{FRM}. \quad (7)$$

Above, $\langle \cdot \rangle_{FRM}$ denotes the average over an ensemble of FRM.

The average over the distribution of level spacings leads to

$$\langle \delta(E - (E_{\alpha} - E_{\beta})) \rangle_{FRM} = \frac{1}{\mathcal{D}(\mathcal{D}-1)} \int \delta(E - (E_1 - E_2)) R_2(E_1, E_2) dE_1 dE_2, \quad (8)$$

where $R_2(E_1, E_2)$ is the Dyson's two-level correlation function [1]. $R_2(E_1, E_2)$ gives the probability for finding a level around the energies E_1 and E_2 . This function can be written as $R_2(E_1, E_2) = R_1(E_1)R_1(E_2) - T_2(E_1, E_2)$, where $R_1(E_1)$ is the density of states and $T_2(E_1, E_2)$ is the two-level cluster function [1].

In FRM, $R_1(E)$ and the LDOS coincide, both having a semicircular form [30–32]. This coincidence is nearly preserved also in realistic many-body models with two-body interactions when the initial state is very delocalized in the energy eigenbasis. However, in this case, the shape of both distributions are Gaussian. The Fourier transform of a Gaussian envelope results in the Gaussian decay of the survival probability, $P_{ini} = \exp(-i\omega_{ini}^2 t^2)$, where

$$\omega_{ini}^2 = \langle \Psi(0) | H^2 | \Psi(0) \rangle - \langle \Psi(0) | H | \Psi(0) \rangle^2 = \sum_{n \neq ini} |\langle \phi_n | H | \phi_{ini} \rangle|^2 \quad (9)$$

is the square of the width of the LDOS. Notice that this is not simply the quadratic decay that develops at very short-times, $t \ll \omega_{ini}^{-1}$, but a true Gaussian behavior that can hold until the inevitable power-law decays develop [39, 40].

The Fourier transform of $T_2(E_1, E_2)$ is directly related to the level number variance [3, 5], a quantity that measures the level of rigidity of the spectrum. Contrary to signatures of chaos associated with the spacings of neighboring levels, the level number variance detects the long-range correlations of the eigenvalues. These correlations are the source of the drop of $P_{ini}(t)$ below $\overline{P_{ini}}$, which is known as correlation hole [43, 45–56]. Manifestations of long-range correlations occur at times of the order of the inverse of the mean level spacing, but still shorter than the Heisenberg time [70]. In the particular case of FRM from GOE, the minimal value reached by $P_{ini}(t)$ due to the correlation hole is $2/\mathcal{D}$ [52].

III. DYNAMICAL MANIFESTATION OF LEVEL REPULSION

We compare results for the integrable XXZ model with those for the chaotic defect and NNN models. To reduce finite size effects, we average the results over different realizations of random numbers representing the small border defects ε_1 and ε_L . We also perform averages over initial states chosen at random among all site-basis vectors. Since the density of states is Gaussian, the majority of these states have energy close to the middle of the spectrum.

A. Growth in Time of the Entanglement and Shannon Entropies

The main panels in Fig. 1 reinforce ideas presented in previous works. They show the evolution of the entanglement entropy (top panels) [Eq. (2)] and of the Shannon entropy (bottom panels) [Eq. (3)] for the XXZ (a,d), defect (b,e)

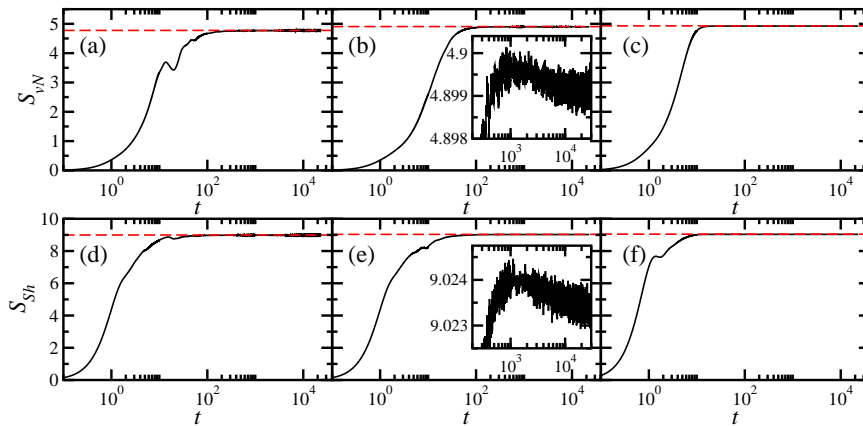


FIG. 1: Evolution of the entanglement entropy (top panels) and Shannon entropy (bottom panels) for the XXZ (a, d), defect (b, e), and NNN (c, f) models. Dashed horizontal lines give the saturation values. The insets in (b) and (e) are zoom ins of the plots at long times. The parameters are $\Delta = 0.48$, $d = 0.9$, $\lambda = 1$, $h = 0$, $L = 16$, $S^z = 0$, $\mathcal{D} = 12\,870$, $\mathcal{D}_A = 256$; open boundaries. Average over 50 initial states corresponding to randomly selected site-basis vectors and average over 20 realizations of random border defects.

and NNN (c,f) models. As described below, the behaviors are very similar for both entropies and for the integrable and chaotic models.

For $t \ll \omega_{ini}^{-1}$, the entropies grow quadratically [31], as expected by simply expanding the expressions in Eq. (2) and Eq. (3). Subsequently, the increase is linear nearly until saturation. The linear increase of the entropies reflects the large number of decay channels available for the initial state, not necessarily the presence of level repulsion. This was stressed in Refs. [18, 21, 22], where clean models were considered, and also in Ref. [19] for disordered systems. In [21, 22], the Shannon entropy was studied for initial states corresponding to mean-field basis vectors. This allowed for the derivation of analytical expressions following the steps discussed in [71]. In [18] both entropies were considered, but only for two specific site-basis vectors, the Néel state and the domain wall state. Here, we average the results over 50 different site-basis vectors and also over 20 realizations of random border defects, so the curves are smoother.

The fact that both entropies lead to very similar behaviors suggests that any of the two can be equivalently used to study nonequilibrium quantum dynamics. In this context, entanglement does not appear to be an essential property [67, 72]. The advantage of the Shannon entropy is to be computationally less expensive, since it does not require the partial trace. It would be interesting, however, to identify which features of the dynamics of many-body quantum systems one entropy can detect that the other cannot.

At first sight, the results for the entropies in the main panels of Fig. 1 seem unable to differentiate integrable from chaotic models. However, the Shannon entropy explicitly contains the survival probability,

$$S_{Sh}(t) = -P_{ini}(t) \ln P_{ini}(t) - \sum_{n \neq ini} P_n(t) \ln P_n(t), \quad (10)$$

so one might expect that it could capture some signature of level repulsion. Specifically, in the time interval where the correlation hole takes place for the survival probability, Eq. (10) suggests that an increase beyond the saturation value for the Shannon entropy could happen. By substantially zooming in the results at long times, we indeed find such bulge. It is visible for both entropies in the defect model, as shown in the insets of Fig. 1 (b) and (e), but no sign of it appears in the integrable XXZ model.

B. Emergence of the Correlation Hole

The survival probability is a very simple quantity that contains a lot of information about the system and its evolution at different time scales. When systems with two-body interactions are strongly perturbed out of equilibrium, as in the cases where site-basis vectors evolve under the XXZ, defect, and NNN models, the envelope of the LDOS is Gaussian and the initial decay of the survival probability is also Gaussian [30–32]. This is illustrated in Fig. 2 for the three models: XXZ (a,d), defect (b,e) and NNN (c,f). This behavior persists up to $t \sim 2$. Between $t \sim 2$ and $t \sim 10$, there are oscillations most likely associated with finite size effects and the energy bounds of the spectrum [39, 40]. They lead to values of $P_{ini}(t)$ below the saturation line, but they are not yet related to the correlation hole. In the examples of Fig. 2, these drops are more significant for the clean XXZ and NNN models than for the defect model.

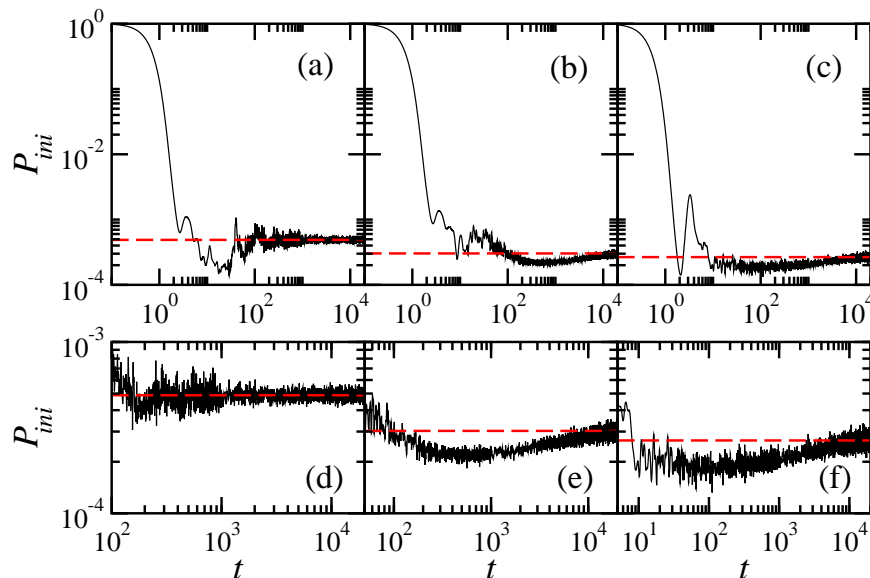


FIG. 2: Survival probability for the XXZ (a,d), defect (b,e), and NNN (c,f) models. The parameters are $\Delta = 0.48$, $d = 0.9$, $\lambda = 1$, $h = 0$, $L = 16$, $S^z = 0$, $\mathcal{D} = 12\,870$. Average over 50 initial states corresponding to randomly selected site-basis vectors and average over 20 realizations of random border defects.

Due to the energy bounds in the spectrum, the initial Gaussian decay gives place to a power-law decay at later times. For small system sizes, this behavior is noticeable in disordered models [19, 39, 40], where averages over several disorder realizations and initial states are performed. The power-law decay is not visible in Fig. 2, probably because of large finite size effects, but the small values of $P_{ini}(t) < \overline{P_{ini}}$ for $t \lesssim 10$ may be an indication that it was at the verge of appearance. In the vicinity of the point where the decay of the survival probability changes from Gaussian to power-law, there occurs an interference between the two contributions. This causes a phenomenon known as survival collapse [41, 73, 74] that often results in $P_{ini}(t) < \overline{P_{ini}}$, as indeed confirmed for spin-1/2 systems in Ref. [40].

It is for times even longer, $t > 10$, that the correlation hole finally develops, first for the NNN model, where the minimum occurs at $t \sim 111$ for the parameters of Fig. 2, and later for the defect model, where the minimum is at $t \sim 564$. The energy range of the spectrum of the NNN model is broader than for the defect model, while both have the same number of levels for the same system size. Since the time for the emergence of the correlation hole is related to the inverse of the mean level spacing, this explains why the hole emerges earlier for the NNN model. By comparing Fig. 2 (e) and the inset of Fig. 1 (e), we also notice that the maximum value in the bulge of the Shannon entropy occurs at a time of the same order of magnitude as the time for the minimum of the correlation hole.

After the correlation hole, the survival probability simply fluctuates around the saturation point, $\overline{P_{ini}}$. The fluctuations tend to be smaller in chaotic models [compare Fig. 2 (d) and Fig. 2 (e)], but they decrease with system size in a similar way for chaotic and interacting integrable models [11].

IV. TRANSITION TO THE MANY-BODY LOCALIZED PHASE

In the interacting disordered spin-1/2 model with $h \neq 0$ and $\lambda = 0$, a transition region between the chaotic delocalized phase and the localized phase in space emerges when the disorder strength gets larger than the coupling strength, $h > 1$. In this region, the level statistics is intermediate and the eigenstates are multifractal [19]. We deal with extended nonergodic eigenstates that become more correlated as h increases. These correlations are responsible for the logarithmic growth of the entanglement [34, 35] and Shannon entropies [19], and for the power-law decays of local observables [75, 76], the out-of-time correlators [77], and the survival probability with exponents smaller than 1 [19, 37]. It was shown in Refs. [19, 37] that $S_{Sh,vN}(t) \sim D_2 \ln(t)$ and $W_{ini}(t) \propto t^{-D_2}$, where D_2 is the fractal dimension obtained from scaling analysis of the participation ratio of the initial state projected into the energy eigenbasis. D_2 also agrees with the fractal dimension obtained from scaling analysis of the participation ratio of the eigenstates written in the site-basis vectors.

Since the delocalized-localized transition in disordered models with interactions happens in parallel with the transition from a Wigner-Dyson to a Poisson distribution [67], we can use the disappearance of level repulsion to capture the transition to the many-body localized phase. One way to do this is by computing the eigenvalues to directly study

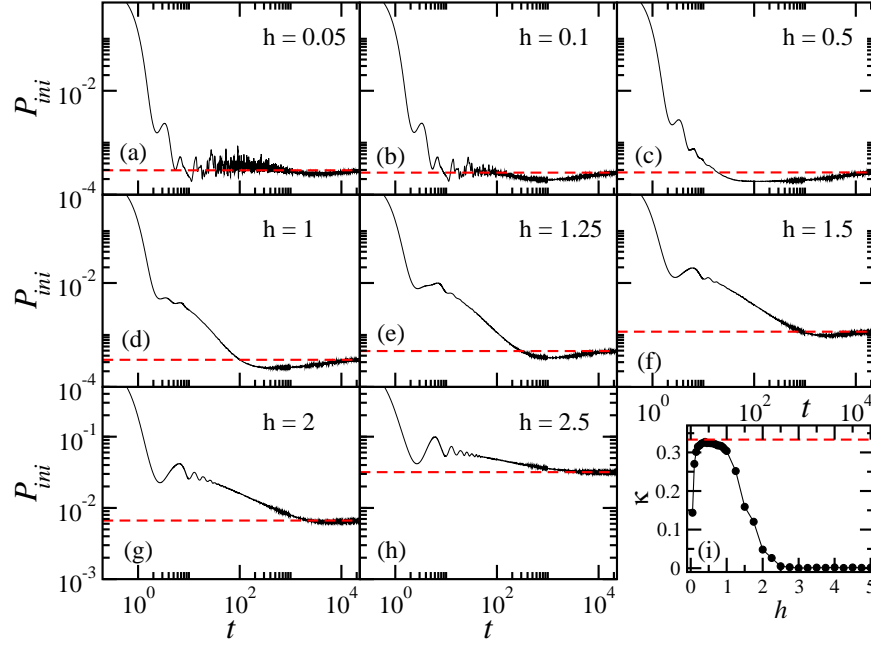


FIG. 3: Survival probability up to saturation (a)-(h) and the depth κ of the correlation hole *vs.* disorder strength (i). The values of h are indicated in the figure; $\Delta = 1$, $\varepsilon_{1,L}, d, \lambda = 0$, $L = 16$, $S^z = 0$. The dashed-lines in (a)-(h) indicate the infinite-time average, $\overline{P_{ini}}$ and in (i) it is the maximum $\kappa = 1/3$ reached by FRM. Average performed over $\sim 10^3$ different initial states corresponding to site-basis vectors with energy in the middle of the spectrum and over 10^2 disorder realizations.

level statistics. The other is by analyzing the evolution of the survival probability and how the correlation hole fades away as the disorder strength becomes large. The latter is the approach taken here.

Figure 3 shows the survival probability for different values of h . The decay is Gaussian at short times and then becomes power-law. In the intermediate region between the chaotic limit and the many-body localized phase, the Fourier transform of the autocorrelation function in Eq. (5), $G(E) \propto E^{D_2-1}$, leads to the power-law decay with exponent $D_2 < 1$. This exponent reflects the level of correlations of the eigenstates [19, 37], as mentioned above. In the chaotic regime, the power-law exponent is larger than 1 and can no longer be explained in terms of the correlations between eigenstates. The power-law decay is now associated with the inevitable presence of energy bounds in the spectrum of quantum systems [39, 40]. By taking these bounds into account when performing the Fourier transform of a Gaussian LDOS in Eq. (4), we find the maximum value 2 for the power-law exponent.

At long times, beyond the power-law decay and before the saturation of $P_{ini}(t)$, the correlation hole emerges when the spectrum shows level repulsion. In Fig. 3 (a), where the disorder strength is very small and the system is close to the delocalized integrable XXZ model, one hardly sees the hole. It gets deeper as h increases from zero. The maximum level of chaoticity, in the sense of proximity to the Wigner-Dyson distribution, happens at $h \sim 0.5$ for the system size considered here. At this point, the correlation hole is deepest [Fig. 3 (c)]. For even larger h , the hole starts shrinking once again. As level repulsion gradually gives space to level crossing, from Fig. 3 (c) to Fig. 3 (h), the correlation hole gets postponed to later times.

To quantify the depth of the correlation hole, we calculate

$$\kappa = \frac{\overline{P_{ini}} - \langle P_{ini}^{min} \rangle}{\overline{P_{ini}}}, \quad (11)$$

where $\langle P_{ini}^{min} \rangle$ is the minimum value of $P_{ini}(t)$. For FRM of GOE, $\kappa_{FRM} = 1/3$. Figure 3 (i) shows κ as a function of the disorder strength. It reaches the largest values in the chaotic region ($h \sim 0.5$), where it approaches κ_{FRM} . It decreases for $h < 0.5$, as the system approaches integrability, and for $h > 0.5$, as the system approaches localization. The depth of the correlation is therefore a general indicator of the integrable-chaos transition, which captures also the delocalized-localized transition.

V. CONCLUSION

We analyzed how the presence of level repulsion manifests itself in the dynamics of many-body quantum systems. We showed that it appears in the form of a correlation hole in the long-time evolution of the survival probability and as a minor bulge above the saturation values of the Shannon and entanglement entropies. The correlation hole can be used to identify the integrable-chaos transition in clean and disordered models as well as the delocalized-localized transition in interacting systems with onsite disorder.

Since the correlation hole reveals the statistical properties of the spectrum from the time domain, it is advantageous to experiments that have low energy resolution and to experiments that do not have direct access to the energy levels. The hole was observed in molecules, but would require long-time coherences to be seen in experiments with cold atoms and trapped ions.

It is worth emphasizing once again the similarities between the dynamical behavior of the Shannon entropy and the entanglement entropy in clean and disordered systems. The entanglement entropy is not only computationally more involved, but also experimentally challenging. The Shannon entropy should be a more accessible quantity to current experiments that investigate nonequilibrium quantum dynamics.

Acknowledgments

EJTH acknowledges funding from PRODEP-SEP and Proyectos VIEP-BUAP, Mexico. EJTH thanks the LNS-BUAP for allowing use of their supercomputing facility and the Aspen Center for Physics hospitality, where part of this work was done. LFS thanks Antonio Garcia-Garcia for very fruitful discussions. LFS was supported by the NSF grant No. DMR-1603418.

-
- [1] M. L. Mehta, *Random Matrices* (Academic Press, Boston, 1991).
 - [2] T. A. Brody, J. Flores, J. B. French, P. A. Mello, A. Pandey, and S. S. M. Wong, *Rev. Mod. Phys.* **53**, 385 (1981).
 - [3] T. Guhr, A. Mueller-Gröeling, and H. A. Weidenmüller, *Phys. Rep.* **299**, 189 (1998).
 - [4] V. Zelevinsky, B. A. Brown, N. Frazier, and M. Horoi, *Phys. Rep.* **276**, 85 (1996).
 - [5] H.-J. Stöckmann, *Quantum Chaos: An Introduction* (Cambridge University Press, Cambridge, 2006).
 - [6] E. P. Wigner, *Proc. Cambridge Phil. Soc.* **47**, 790 (1951).
 - [7] E. P. Wigner, *Ann. Math.* **67**, 325 (1958).
 - [8] A. Peres, *Phys. Rev. A* **30**, 1610 (1984).
 - [9] P. Reimann, *Phys. Rev. Lett.* **101**, 190403 (2008).
 - [10] A. J. Short, *New J. Phys.* **13**, 053009 (2011).
 - [11] P. R. Zangara, A. D. Dente, E. J. Torres-Herrera, H. M. Pastawski, A. Iucci, and L. F. Santos, *Phys. Rev. E* **88**, 032913 (2013).
 - [12] T. Kiendl and F. Marquardt, arXiv:1603.01071.
 - [13] F. Borgonovi, F. M. Izrailev, L. F. Santos, and V. G. Zelevinsky, *Phys. Rep.* **626**, 1 (2016).
 - [14] L. D'Alessio, Y. Kafri, A. Polkovnikov, and M. Rigol, *Advances in Physics* **65**, 239 (2016).
 - [15] M. Rigol and M. Srednicki, *Phys. Rev. Lett.* **108**, 110601 (2012).
 - [16] E. J. Torres-Herrera and L. F. Santos, *Phys. Rev. E* **88**, 042121 (2013).
 - [17] J. Eisert, M. Cramer, and M. B. Plenio, *Rev. Mod. Phys.* **82**, 277 (2010).
 - [18] E. J. Torres-Herrera, J. Karp, M. Távora, and L. F. Santos, *Entropy* **18**, 359 (2016).
 - [19] E. J. Torres-Herrera and L. F. Santos, *Annalen der Physik* p. 1600284 (2017).
 - [20] V. Balachandran, G. Benenti, G. Casati, and J. Gong, *Phys. Rev. E* **82**, 046216 (2010).
 - [21] L. F. Santos, F. Borgonovi, and F. M. Izrailev, *Phys. Rev. Lett.* **108**, 094102 (2012).
 - [22] L. F. Santos, F. Borgonovi, and F. M. Izrailev, *Phys. Rev. E* **85**, 036209 (2012).
 - [23] P. Jacquod, P. Silvestrov, and C. Beenakker, *Phys. Rev. E* **64**, 055203 (2001).
 - [24] F. M. Cucchietti, C. H. Lewenkopf, E. R. Mucciolo, H. M. Pastawski, and R. O. Vallejos, *Phys. Rev. E* **65**, 046209 (2002).
 - [25] T. Prosen, *Phys. Rev. E* **65**, 036208 (2002).
 - [26] Y. S. Weinstein, J. Emerson, S. Lloyd, and D. Cory, *Quant. Inf. Proc.* **1**, 439 (2003).
 - [27] E. J. Torres-Herrera and L. F. Santos, in *AIP Proceedings*, edited by P. Danielewicz and V. Zelevinsky (APS, East Lansing, Michigan, 2014).
 - [28] V. V. Flambaum and F. M. Izrailev, *Phys. Rev. E* **64**, 026124 (2001).
 - [29] V. K. B. Kota, *Lecture Notes in Physics, vol. 884* (Springer, Heidelberg, 2014).
 - [30] E. J. Torres-Herrera and L. F. Santos, *Phys. Rev. A* **89**, 043620 (2014).
 - [31] E. J. Torres-Herrera, M. Vyas, and L. F. Santos, *New J. Phys.* **16**, 063010 (2014).
 - [32] E. J. Torres-Herrera and L. F. Santos, *Phys. Rev. A* **90**, 033623 (2014).
 - [33] E. J. Torres-Herrera, D. Kollmar, and L. F. Santos, *Phys. Scr. T* **165**, 014018 (2016).

- [34] M. Žnidarič, T. Prosen, and P. Prelovšek, Phys. Rev. B **77**, 064426 (2008).
- [35] J. H. Bardarson, F. Pollmann, and J. E. Moore, Phys. Rev. Lett. **109**, 017202 (2012).
- [36] D. J. Luitz and Y. B. Lev, arXiv:1607.01012.
- [37] E. J. Torres-Herrera and L. F. Santos, Phys. Rev. B **92**, 014208 (2015).
- [38] E. J. Torres-Herrera, M. Távora, and L. F. Santos, Braz. J. Phys. **46**, 239 (2016).
- [39] M. Távora, E. J. Torres-Herrera, and L. F. Santos, Phys. Rev. A **94**, 041603 (2016).
- [40] M. Távora, E. J. Torres-Herrera, and L. F. Santos, Phys. Rev. A **95**, 013604 (2017).
- [41] J. G. Muga, A. Ruschhaupt, and A. del Campo, *Time in Quantum Mechanics, vol. 2* (Springer, London, 2009).
- [42] A. del Campo, New J. Phys. **18**, 015014 (2016).
- [43] L. Leviandier, M. Lombardi, R. Jost, and J. P. Pique, Phys. Rev. Lett. **56**, 2449 (1986).
- [44] J. S. Cotler, G. Gur-Ari, M. Hanada, J. Polchinski, P. Saad, S. H. Shenker, D. Stanford, A. Streicher, and M. Tezuka, arXiv:1611.04650.
- [45] J. P. Pique, Y. Chen, R. W. Field, and J. L. Kinsey, Phys. Rev. Lett. **58**, 475 (1987).
- [46] T. Guhr and H. Weidenmüller, Chem. Phys. **146**, 21 (1990), ISSN 0301-0104.
- [47] M. Lombardi and T. H. Seligman, Phys. Rev. A **47**, 3571 (1993).
- [48] L. Michaille and J.-P. Pique, Phys. Rev. Lett. **82**, 2083 (1999).
- [49] Y. Alhassid, Y. V. Fyodorov, T. Gorin, W. Ihra, and B. Mehlh, Phys. Rev. A **73**, 042711 (2006).
- [50] U. Hartmann, H. Weidenmüller, and T. Guhr, Chem. Phys. **150**, 311 (1991), ISSN 0301-0104.
- [51] A. Delon, R. Jost, and M. Lombardi, J. Chem. Phys. **95**, 5701 (1991).
- [52] Y. Alhassid and R. D. Levine, Phys. Rev. A **46**, 4650 (1992).
- [53] T. Gorin, T. Prosen, and T. H. Seligman, New J. Phys. **6**, 20 (2004).
- [54] F. Leyvraz, A. García, H. Kohler, and T. H. Seligman, J. Phys. A **46**, 275303 (2013).
- [55] A. Kudrolli, S. Sridhar, A. Pandey, and R. Ramaswamy, Phys. Rev. E **49**, R11 (1994).
- [56] H. Alt, H.-D. Gräf, T. Guhr, H. L. Harney, R. Hofferbert, H. Rehfeld, A. Richter, and P. Schardt, Phys. Rev. E **55**, 6674 (1997).
- [57] B. V. Chirikov, Physics Letters A **108**, 68 (1985), ISSN 0375-9601.
- [58] B. Chirikov, Open Systems & Information Dynamics **4**, 241 (1997), ISSN 1573-1324.
- [59] F. C. Alcaraz, M. N. Barber, M. T. Batchelor, R. J. Baxter, and G. R. W. Quispel, J. Phys. A **20**, 6397 (1987).
- [60] L. F. Santos, J. Phys. A **37**, 4723 (2004).
- [61] E. J. Torres-Herrera and L. F. Santos, Phys. Rev. E **89**, 062110 (2014).
- [62] T. C. Hsu and J. C. A. d'Auriac, Phys. Rev. B **47**, 14291 (1993).
- [63] K. Kudo and T. Deguchi, J. Phys. Soc. Jpn. **74**, 1992 (2005).
- [64] L. F. Santos, J. Math. Phys. **50**, 095211 (2009).
- [65] A. Gubin and L. F. Santos, Am. J. Phys. **80**, 246 (2012).
- [66] Y. Avishai, J. Richert, and R. Berkovitz, Phys. Rev. B **66**, 052416 (2002).
- [67] L. F. Santos, G. Rigolin, and C. O. Escobar, Phys. Rev. A **69**, 042304 (2004).
- [68] F. Dukesz, M. Zilbergerts, and L. F. Santos, New J. Phys. **11**, 043026 (2009).
- [69] L. Amico, R. Fazio, A. Osterloh, and V. Vedral, Rev. Mod. Phys. **80**, 517 (2008).
- [70] A. M. García-García and J. J. M. Verbaarschot, Phys. Rev. D **94**, 126010 (2016).
- [71] V. V. Flambaum and F. M. Izrailev, Phys. Rev. E **64**, 036220 (2001).
- [72] W. G. Brown, L. F. Santos, D. Starling, and L. Viola, Phys. Rev. E **77**, 021106 (2008).
- [73] E. Rufeil-Fiori and H. Pastawski, Chem. Phys. Lett. **420**, 35 (2006).
- [74] E. Rufeil-Fiori and H. Pastawski, Physica B **404**, 2812 (2009).
- [75] M. Serbyn, Z. Papić, and D. A. Abanin, Phys. Rev. B **90**, 174302 (2014).
- [76] D. J. Luitz, N. Laflorencie, and F. Alet, Phys. Rev. B **93**, 060201 (2016).
- [77] R. Fan, P. Zhang, H. Shen, and H. Zhai, arXiv:1608.01914.